Dielectric materials for electronic

Présentée par:
BENNACER Hamza

les diélectriques.

Les diélectriques sont une classe importante de matériaux électroniques et notamment pour la microélectronique et l'optoélectronique. Les applications incluent un large éventail d'applications de dispositifs, y compris des dispositifs actifs tels que **les transistors** et leur isolation électrique, ainsi que des dispositifs passifs, tels que des **condensateurs**.

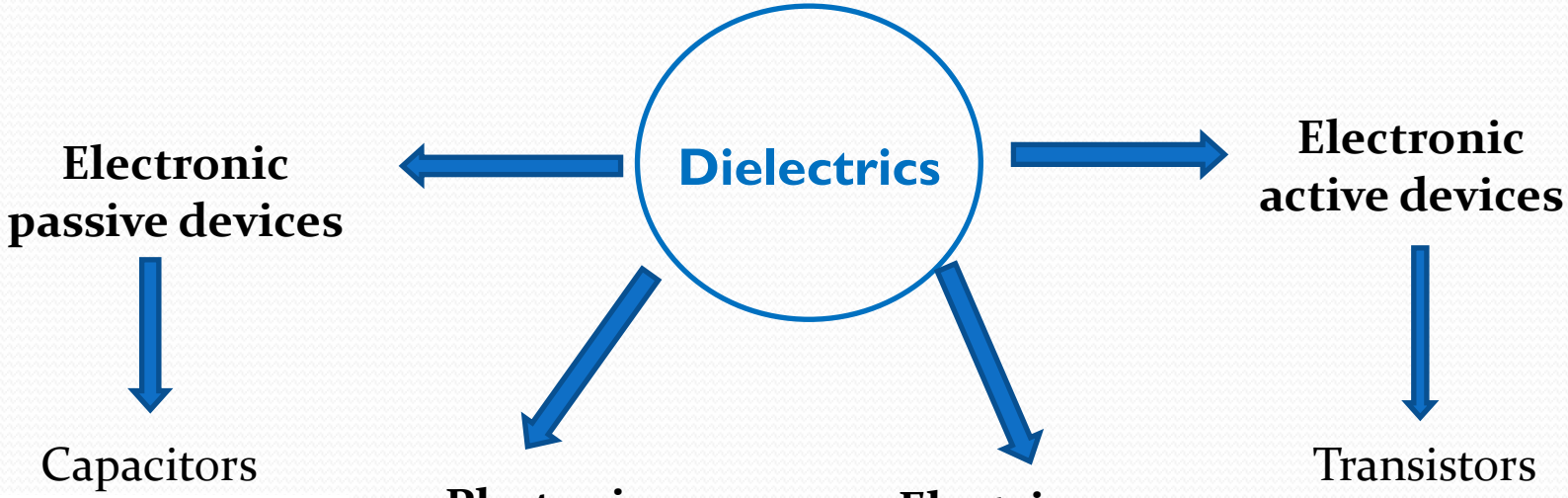

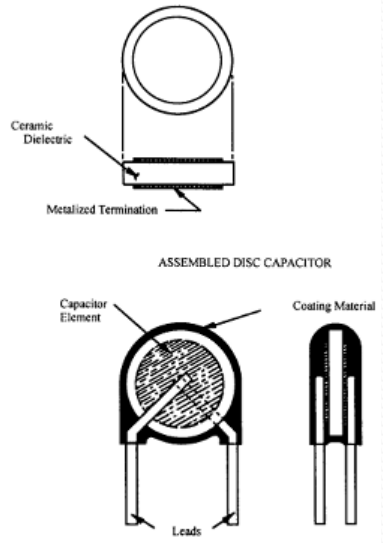

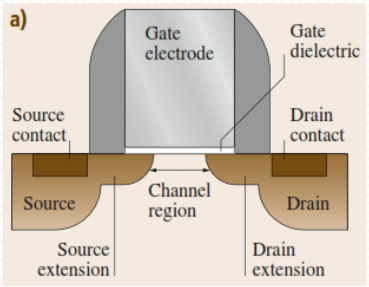

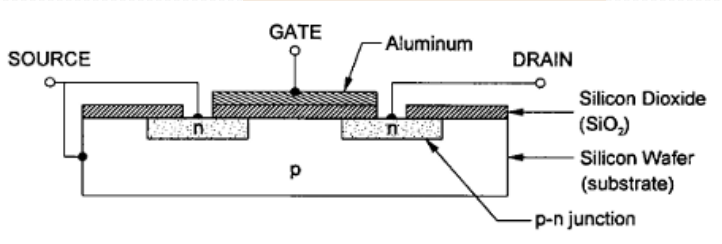

les diélectriques.

- Les diélectriques sont omniprésents dans toute la structure de un circuit intégré. Les applications incluent les diélectriques de grille, oxydes tunnel dans les dispositifs de mémoire, condensateur diélectriques, diélectriques d'interconnexion et isolation les diélectriques, ainsi que les applications sacrificielles ou de masquage pendant le processus de fabrication du circuit.

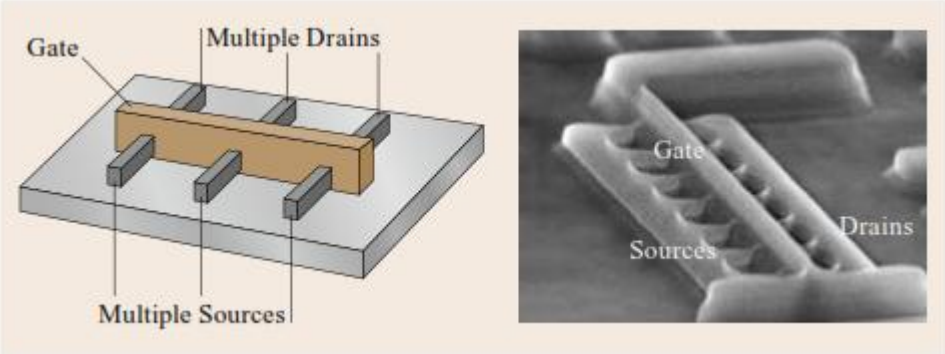

Trigate transistor structure [*]

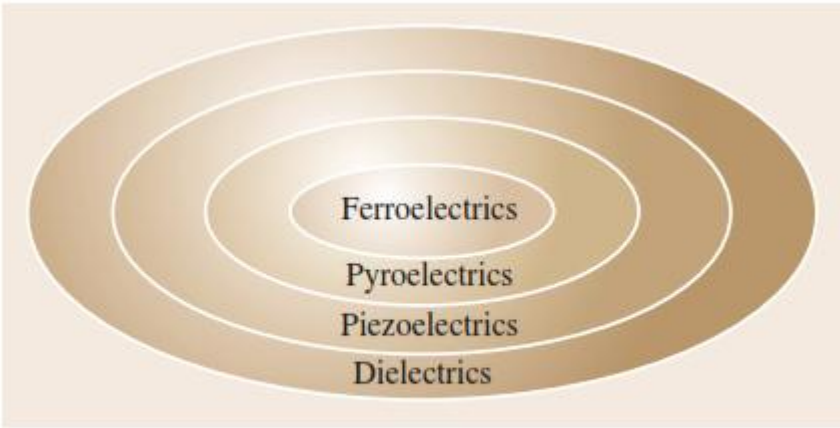

Fig. 26.1 Venn diagram showing how ferroelectrics fit into the different classes of dielectric materials

- Un milieu est diélectrique, s'il ne contient pas de charges électriques susceptibles de se déplacer de façon macroscopique. Le milieu ne peut donc pas conduire le courant électrique, donc, par définition un isolant électrique. Quelques exemples de milieux diélectriques : le vide, le verre, le bois sec, de nombreux plastiques, etc…

ZnO
Zinc d'oxide

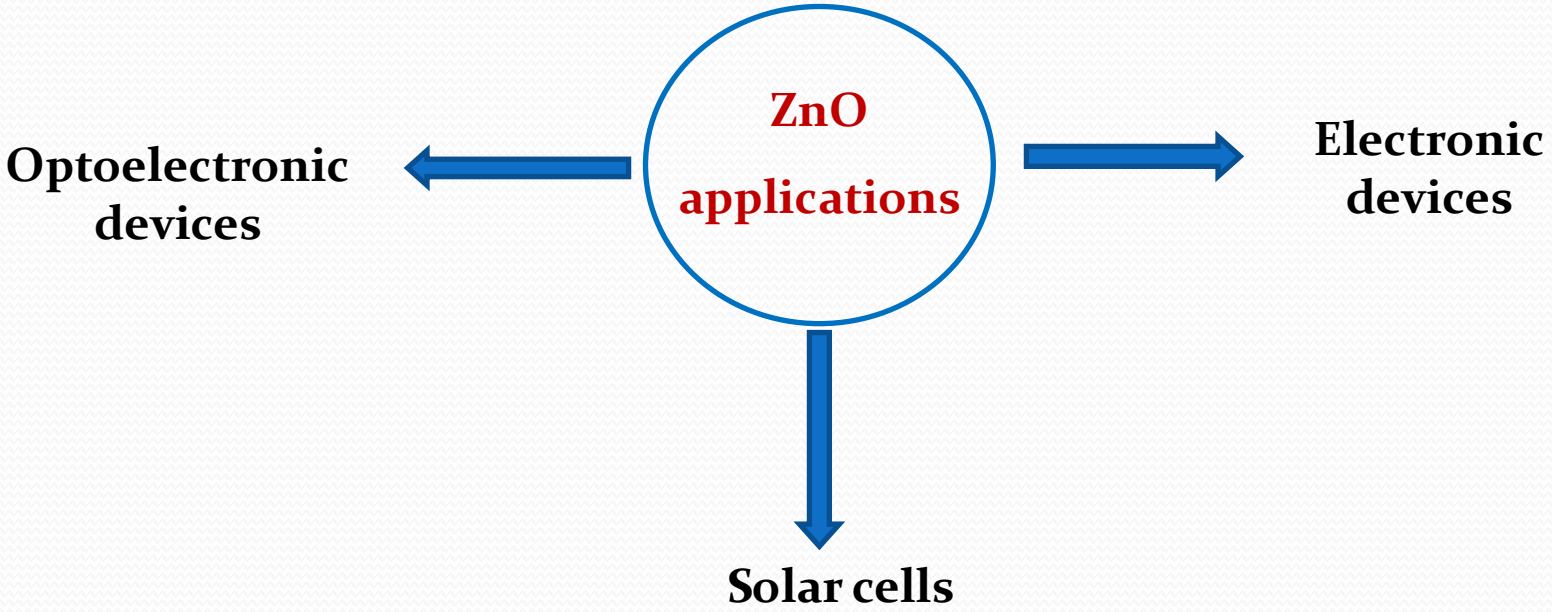

Advantages of ZnO:

- large bandgap include high-temperature and high-power operation,
- lower noise generation,
- higher breakdown voltages,
- and ability to sustain large electric fields.

ZnO
Zinc d'oxide

Most of the group **II–VI** binary compound crystallize in either **cubic zinc blende** or **hexagonal wurtzite** (Wz) structure.

II-VI

ZnO **MgO**

12 IIB	13 IIIA	14 IVA	15 VA	16 VIA
	5 10.811 **B** BORE	6 12.011 **C** CARBONE	7 14.007 **N** AZOTE	8 15.999 **O** OXYGÈNE
	13 26.982 **Al** ALUMINIUM	14 28.086 **Si** SILICIUM	15 30.974 **P** PHOSPHORE	16 32.065 **S** SOUFRE
30 65.38 **Zn** ZINC	31 69.723 **Ga** GALLIUM	32 72.64 **Ge** GERMANIUM	33 74.922 **As** ARSENIC	34 78.96 **Se** SÉLÉNIUM

covalent bonding nature
Or
a substantial ionic character

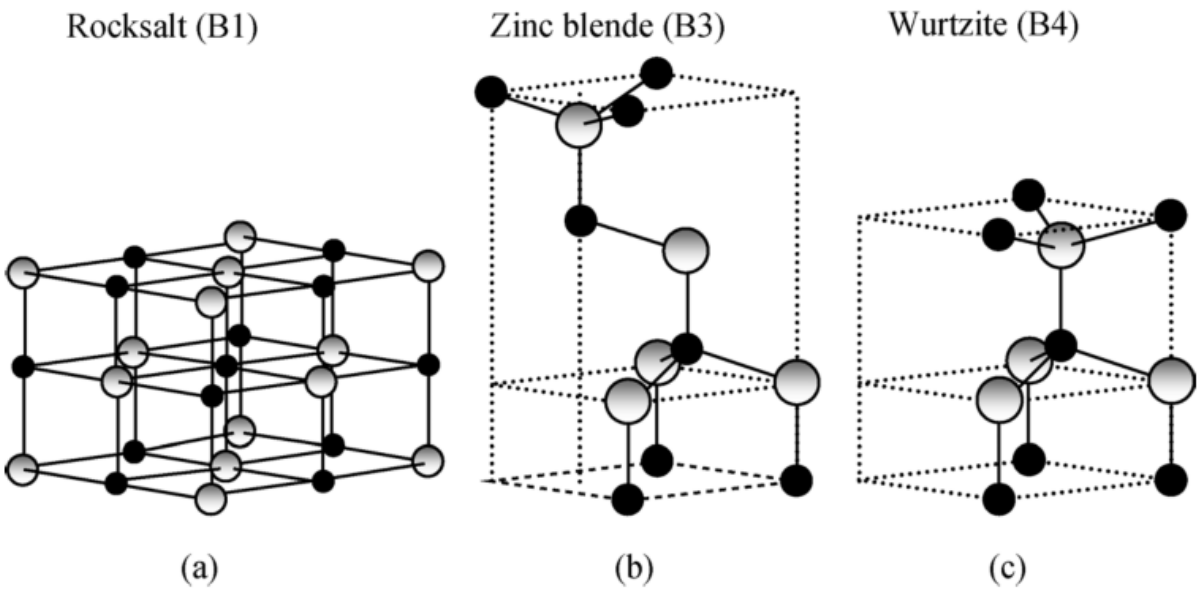

Figure 1.1 Stick-and-ball representation of ZnO crystal structures: (a) cubic rocksalt (B1), (b) cubic zinc blende (B3), and (c) hexagonal wurtzite (B4). Shaded gray and black spheres denote Zn and O atoms, respectively.

ZnO
Zinc d'oxide

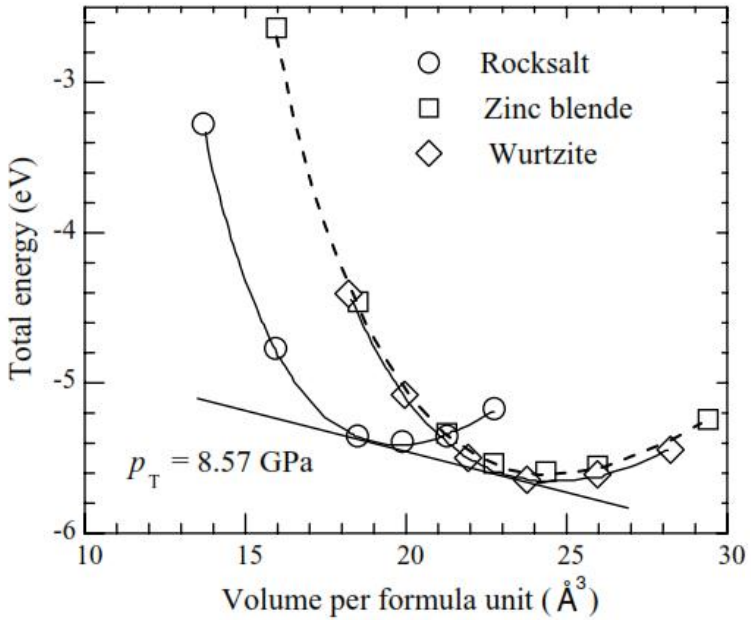

Figure 1.9 Total energy versus volume (both per ZnO formula unit) for the three phases: zinc blende (squares), wurtzite (diamonds), and rocksalt (circles). The zero of energy is the sum of the total energies of an isolated Zn and an isolated O atom. The hexagonal/cubic phase transition occurs at $p_T = 8.57$ GPa. (After Ref. [20].)

Table 1.2 Measured and calculated lattice constants and the *u* parameter of ZnO.

Wurtzite				
a **(Å)**	***c*** **(Å)**	***c/a***	***u***	**Reference**
		1.633	0.375	Ideal
3.2496	5.2042	1.6018	0.3819	*a*
3.2501	5.2071	1.6021	0.3817	*b*
3.286	5.241	1.595	0.383	*c*
3.2498	5.2066	1.6021		*d*
3.2475	5.2075	1.6035		*e*
3.2497	5.206	1.602		*f*
		1.593	0.3856	*g*
		1.600	0.383	*h*

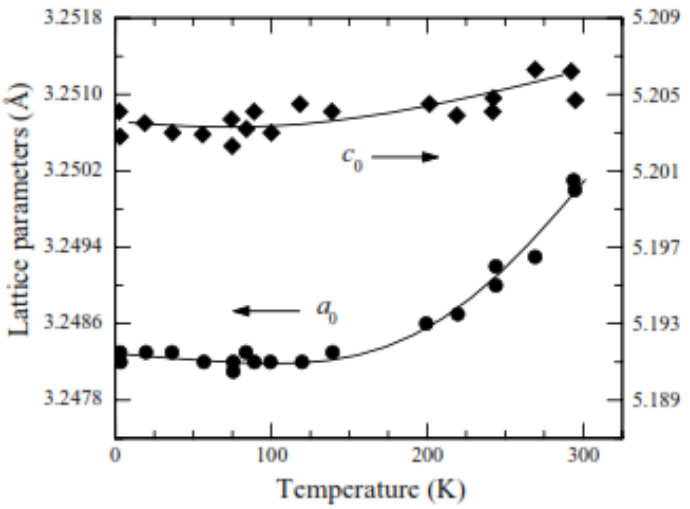

ZnO
Zinc d'oxide

Electronic Band Structure

Table 1.3 Calculated and measured energy gaps E_g, cation d-band positions E_d, and anion p valence bandwidths W_p (all in eV) of ZnO.

	LDA-PP	LDA-SIC-PP	Experiment
E_g	0.23	3.77	3.4
E_d	−5.1	−8.9	−7.8
W_p	−3.99	−5.2	−5.3

After Ref. [48]. LDA-PP: local density approximation – pseudopotential. LDA-SIC-PP: local density approximation – self-interaction corrected pseudopotential.

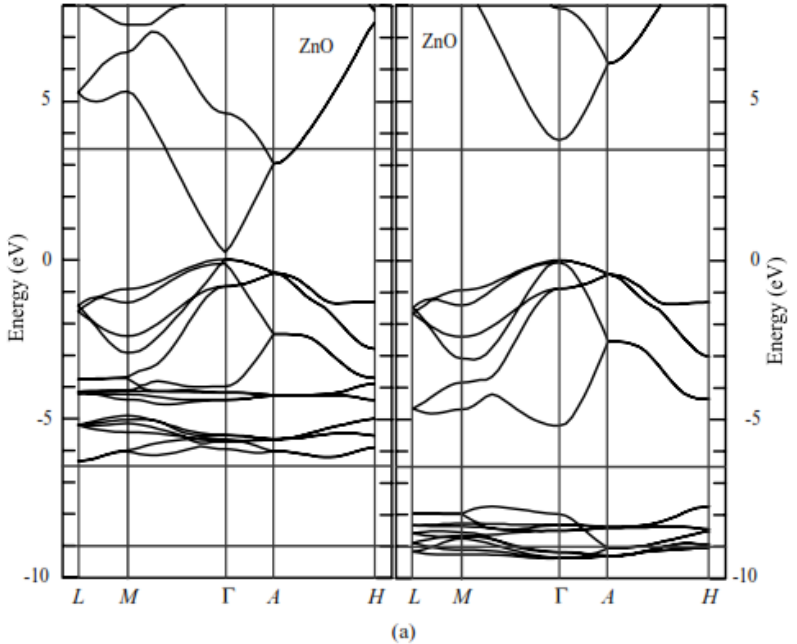

Figure 1.12 (a) LDA bulk band structure of ZnO as calculated by using a standard pseudopotential (PP) (left panel) and by using SIC-PP (right panel). The horizontal dashed lines indicate the measured gap energy and d-band width. (b) Comparison of calculated and measured valence bands of ZnO. The left panel shows the standard LDA, while the right panel shows SIC-PP results. (Courtesy of J. Pollmann [48].)

ZnO
Zinc d'oxide

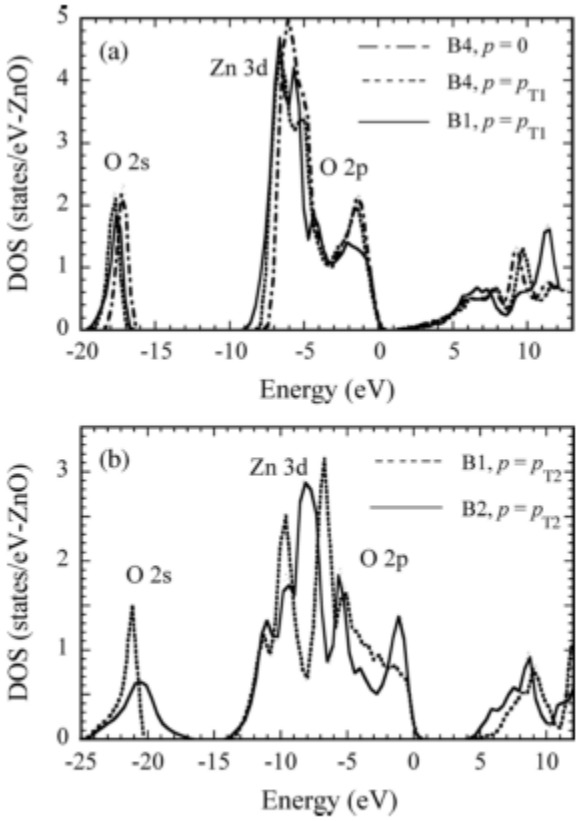

Figure 1.15 Total density of states for ZnO in the (a) B4 structure at $p = 0$ and $p = p_{T1}$ and B1 structure at $p = p_{T1}$, and (b) B1 and B2 structures at $p = p_{T2}$. (Courtesy of J.E. Jaffe [18].)

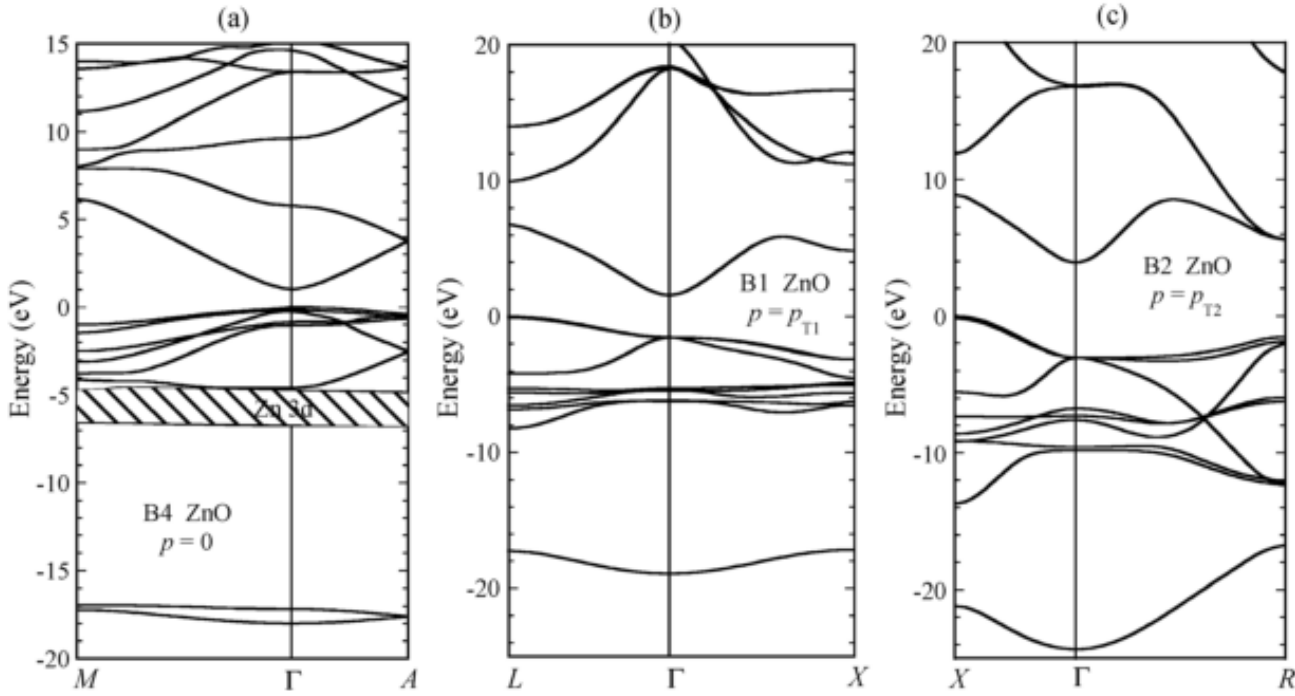

Figure 1.14 Band structure for ZnO: (a) B4 structure at $p = 0$, (b) B1 structure at $p = p_{T1}$, (c) B2 structure at $p = p_{T2}$. (Courtesy of J.E. Jaffe [18].)

ZnO
Zinc d'oxide

Electrical Properties of Undoped ZnO

Sample	Electron mobility ($cm^2 V^{-1} s^{-1}$)	References	Carrier concentration (cm^{-3})
Monte Carlo calculation	300	[158]	—
Bulk ZnO grown by vapor-phase transport method	205	[159]	6.0×10^{16}
Bulk ZnO grown by pressurized melt method	131 (296 K), 298 (77 K)	[160]	5.05×10^{17} (296 K), 3.64×10^{16} (77 K)
Bulk ZnO grown by hydrothermal method	200	[161]	8×10^{13} (Li compensated)
ZnO thin films grown on *c*-plane sapphire substrates by PLD	155	[162]	2.0×10^{16}
ZnO thin films grown on *c*-plane sapphire grown by MBE	130	[163]	1.2×10^{17}
ZnO thin films grown on *a*-plane sapphire by MBE	120	[164]	7.0×10^{16}
$Zn_{0.9}Mn_{0.1}O$/ZnO heterostructure grown on *c*-plane sapphire by PLD	130	[165]	8.8×10^{12} (areal concentration cm^{-3})
ZnO thin films grown on *c*-plane sapphire with ZnO/MgO double-buffer layers grown by MBE	145	[166, 167]	1.2×10^{17}
ZnO thin films grown on MgZnO-buffered $ScAlMgO_4$ substrates by PLD	440	[168]	1×10^{16}

ZnO
Zinc d'oxide

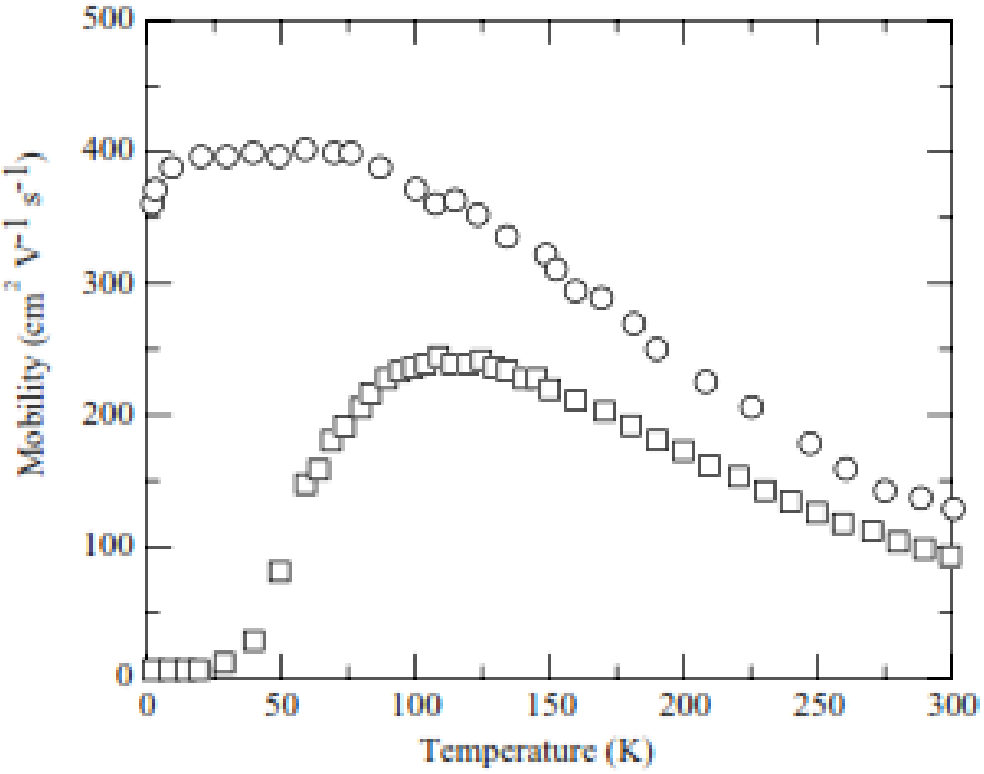

Figure 1.36 Temperature dependence of the mobility of the ZnMnO/ZnO heterostructure (circles) and the 1µm thick ZnO single layer (squares) control sample. (After Ref. [165].)

ZnO
Zinc d'oxide

Table 1.12. Dielectric constant and optical phonon energy (meV) of wurtzite type materials except rocksalt type MgO

	$\varepsilon^{\parallel}(0)$	$\varepsilon^{\perp}(0)$	$\varepsilon^{\parallel}(\infty)$	$\varepsilon^{\perp}(\infty)$	$\hbar\,\omega_{\mathrm{LO}}$	$\hbar\,\omega_{\mathrm{TO}}$
BeO	7.65 [37]	6.94 [37]	2.99 [37]	2.95 [37]	135.2 [37]	87.2 [37]
MgO	9.8 [21]		2.95 [21]		92.2 [21]	49.4 [21]
ZnO	8.49 [38]	7.40 [38]	3.72 [38]	3.68 [38]	72.8 [39]	51.0 [39]

Table 1.5: Static (ϵ_0) and high frequency dielectric constant (ϵ_∞) data for ZnO [40,41].

		Film [41]	Bulk [41]	Bulk [40]
ϵ_0	$E \perp c$	7.46	7.77	
	$E \parallel c$	8.59	8.91	
ϵ_∞	$E \perp c$	3.7	3.6	3.68
	$E \parallel c$	3.78	3.66	3.72

ZnO
Zinc d'oxide

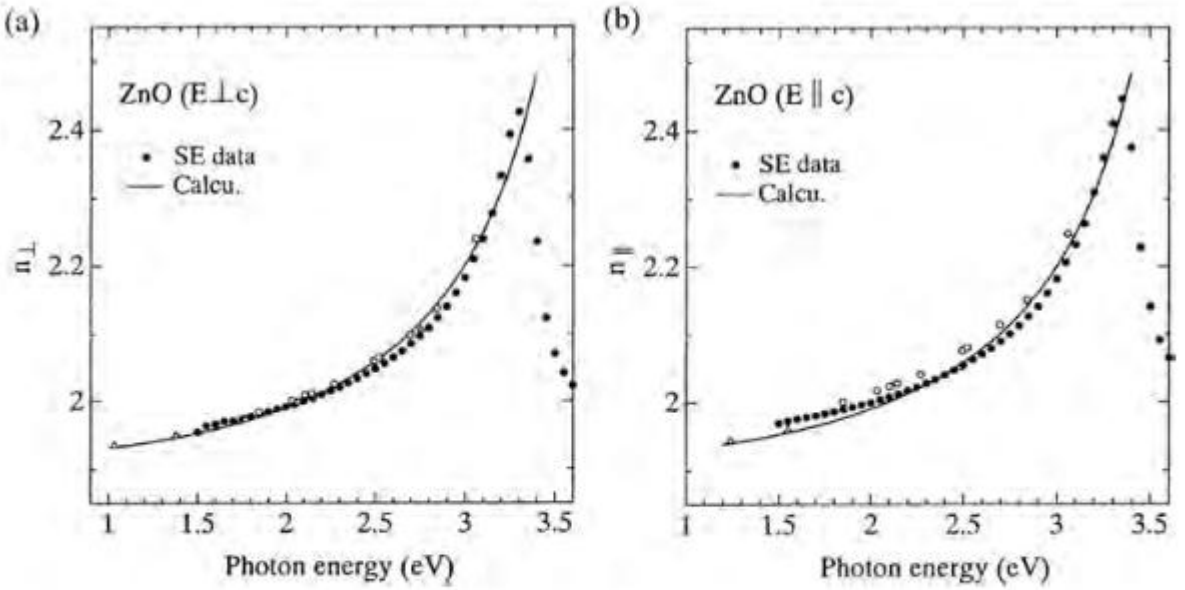

Figure 1.11: Refractive index dispersion of ZnO for E $\perp$ *c* and E $\parallel$ *c* below the fundamental absorption edge. The solid circles represent the spectroscopic ellipsometry data whilst the solid line is calculated data. [Reprinted with permission from H. Yoshikawa and S. Adachi, Jpn. J. Appl. Phys. **36**, 6237 (1997). Copyright 2004 by Jpn. J. Appl. Phys.]

SiO_2

Le SiO_2 est utilisé de façon quasi-incontournable, d'oxyde de grille dans les dispositifs FET (Field Effect Transistors). Dans la structure du MOSFET, l'oxyde de grille (oxyde ou bien diélectrique) isole électriquement la grille et la zone de canal.

Le SiO2 possède plusieurs avantages remarquables :

sa formation naturelle avec le Si

- ❑ une faible densité de défauts dans le volume et à l'interface Si/SiO2 .
- ❑ une haute résistivité électrique (= 10 Ω cm)
- ❑ une large bande interdite (9 eV) …

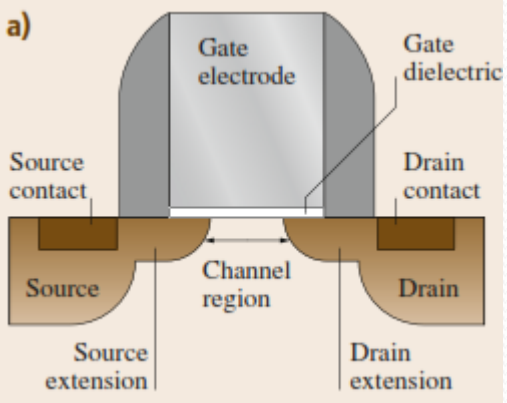

SiO_2

Table 27.2 Properties of SiO_2

Geometrical parameters	
Si—Si bond length	3.12 Å
Si—O bond length	1.62 Å
O—O bond length	2.27 Å
Mean bond angle	144° (tetrahedral bonding)
Bond angle range	Si—O—Si: 110 to 180°
Density (g/cm^3)	
Thermally grown (fused silica)	2.20
Quartz	2.65
Index of refraction (optical frequencies)	
Thermally grown (fused silica)	1.460
Quartz	1.544
Quasi-static dielectric constant (≤ 1 kHz)	
Thermally grown (fused silica)	3.84
Quartz	3.85
Band gap	
Thermally grown (fused silica)	8.9 eV
Quartz	≈ 9.0 eV
Electrical breakdown strength	
Thermally grown (fused silica)	10 MV/cm
Quartz	≈ 10 MV/cm

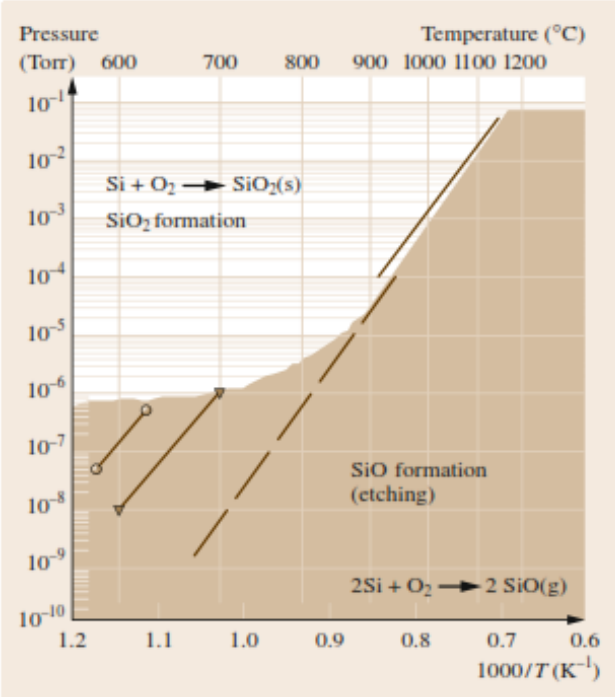

Fig. 27.16 Pressure–temperature phase diagram for thin SiO_2/Si. (After [27.76], © 1997 AIP, with permission)

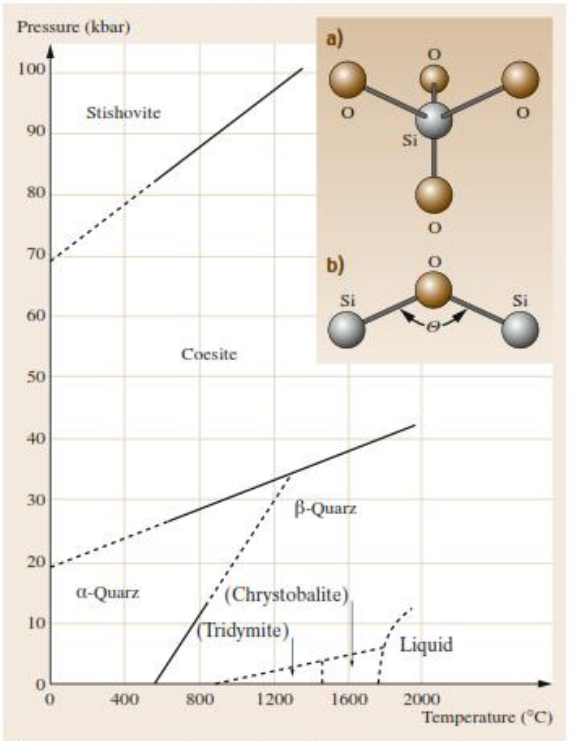

Fig. 27.13a,b Phase diagram for SiO_2. *Inset*: bonding configurations for the O—Si—O system. **(a)** Tetrahedral unit for the Si—O bonding arrangement. **(b)** Bond angle θ defined for O—Si—O bonds. (After [27.41], IOP Publishing © 1994, with permission)

SiO_2

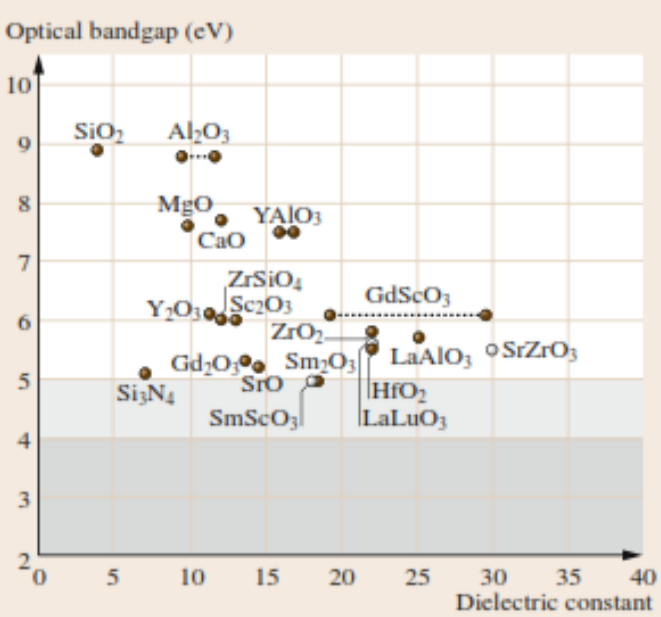

Table 27.4 Comparison of relevant properties for selected high-k candidates. Key: mono. = monoclinic; tetrag. = tetragonal

Material	Dielectric constant (k)	Band gap E_G (eV)	ΔE_C (eV) to Si	Crystal structure(s) (400–1050 °C)
SiO_2	3.9	8.9–9.0	3.2–3.5[b]	Amorphous
Si_3N_4	7	4.8[a] – 5.3	2.4[b]	Amorphous
Al_2O_3	9	6.7[h] – 8.7	2.1[a] – 2.8[b]	Amorphous*
Y_2O_3	11[d] – 15	5.6–6.1[d]	2.3[b]	Cubic
Sc_2O_3	13[d]	6.0[d]		Cubic
ZrO_2	22[d]	5.5[a] – 5.8[d]	1.2[a] – 1.4[b]	Mono., tetrag., cubic
HfO_2	22[d]	5.5[d] – 6.0	1.5[b] – 1.9[c]	Mono., tetrag., cubic
La_2O_3	30	6.0	2.3[b]	Hexagonal, cubic
Ta_2O_5	26	4.6[a]	0.3[a,b]	Orthorhombic
TiO_2	80	3.05–3.3	≈ 0.05[b]	Tetrag. (rutile, anatase)
$ZrSiO_4$	12[d]	6[d] – 6.5	1.5[b]	Tetrag.
$HfSiO_4$	12	6.5	1.5[b]	Tetrag.
$YAlO_3$	16 – 17[d]	7.5[d]		**
$HfAlO_3$	10[e] – 18[g]	5.5–6.4[f]	2–2.3[f]	**
$LaAlO_3$	25[d]	5.7[d]		**
$SrZrO_3$	30[d]	5.5[d]		**
HfSiON	12–17[i,j]	6.9[k]	2.9[k]	Amorphous

* (γ-Al_2O_3 phase) has been recently reported [27.143], ** Onset of crystallization depends upon Al content, [a] [27.144], [b] [27.145–147], [c] [27.148], [d] [27.149], [e] [27.150], [f] [27.148], [g] [27.151], [h] [27.152], [i] [27.153], [j] [27.154], [k] [27.155]